

TWO-QUASIPARTICLE CONFIGURATIONS IN
THE $K^\pi = 0^-$ OCTUPOLE BAND OF $^{238}\text{Pu}^*$

Michael A. Thomason**

Middle Tennessee State University
Murfreesboro, Tennessee

Under the Supervision of:

Arnold M. Friedman

Chemistry Division

Argonne National Laboratory

- * Work performed at Argonne National Laboratory whose facilities are owned by the United States Government. The Laboratory is operated for the U. S. Energy Research and Development Administration by the University of Chicago in accordance with the policies laid down by the Argonne Universities Association.
- ** Participant in the Spring 1975 Undergraduate Research Participation Program, January 13 - May 2, 1975. The program is coordinated by the Argonne Center for Educational Affairs, and is supported by the Division of Physical Research of the U. S. Energy Research and Development Administration.

ABSTRACT

Since single proton transfer reactions pick out individual states, this technique can be used to investigate the make-up of complex vibrational states in heavy, deformed nuclei. The single proton transfer reaction $^{237}\text{Np}(\alpha, t)^{238}\text{Pu}$ has been investigated with 27.5- and 28.0-MeV α particles from the Argonne FN tandem Van de Graaff accelerator. The well-known $K^\pi = 0^-$ octupole band based at 605 keV in ^{238}Pu receives significant population in this reaction. Higher-lying two-proton states are also observed. Utilizing additional data from the $^{239}\text{Pu}(d, t)^{238}\text{Pu}$ reaction, contributions from two-proton and two-neutron configurations to the microscopic composition of the $K^\pi = 0^-$ octupole vibration in ^{238}Pu have been determined.

ACKNOWLEDGEMENTS

It is a pleasure to acknowledge the inspiration and assistance of Arnold Friedman, Steven Yates, and Irshad Ahmad throughout my semester at Argonne.

INTRODUCTION

The nucleon-nucleon interaction is very complex and only partially understood. Nuclei consist of many nucleons and thus *ab initio* calculation of their properties is extremely difficult. For most nuclear problems the approach is simplified by using specific nuclear models combined with simplified nuclear forces.

The shell model^{1,2} successfully accounts for the properties of the particularly stable nuclei with near "magic" numbers³ of protons or neutrons. Nucleons are assumed to move in independent orbits in an average isotropic potential due to all the other nucleons. With the inclusion of a spin-orbit coupling term, solution of the Schroedinger equation results in a nuclear energy level sequence corresponding to the magic numbers of shell closure.

Far from closed shells the nucleus is deformed into a prolate or oblate shape by the coupling of the angular momentum of the core of closed nuclear shells to the angular momenta of the nucleons beyond the last closed shell. The collective theory⁴ explains certain experimentally observed energy levels of deformed nuclei in terms of vibrations of the nucleus about its equilibrium shape. In the classical, idealized case of a nucleus with constant density and a sharp surface the nuclear surface would be defined⁵ by the

$\alpha_{\lambda\mu}$ in the equation,

$$R(\theta\phi) = R_0 \left\{ 1 + \sum_{\lambda\mu} \alpha_{\lambda\mu} Y_{\lambda\mu}(\theta\phi) \right\} \quad (1)$$

The $Y(\theta\phi)$ are spherical harmonics of order λ , while μ is the projection of λ on a space fixed axis and the $\alpha_{\lambda\mu}$ are coefficients.

The shape oscillations may be classified according to their multipole order λ . Frequencies of vibration with $\lambda = 2$ are called quadrupole vibrations, while vibration frequencies with $\lambda = 3$ are called octupole vibrations. Quadrupole vibrations may be further classified by making the substitutions

$$\alpha_{20} = \beta \cos\gamma \quad \text{and} \quad \alpha_{22} = \frac{1}{\sqrt{2}} \beta \sin\gamma$$

Oscillations in the shape parameter β produce β vibrations, while if the parameter γ differs from 0° γ vibrations are produced.

Other experimentally observed energy levels of deformed nuclei are explained by the collective model as rotational states built upon the vibrational and intrinsic nuclear excitations. The energy of the rotational states is given⁶ by the general equation

$$E_I = E_0 + \frac{h^2}{2I} I(I+1) + a(-1)^I + \frac{1}{2}(I + \frac{1}{2})\delta_{K, \frac{1}{2}} \quad (2)$$

where E_0 is a constant depending on the intrinsic structure, I represents the effective moment of inertia about the axis of rotation perpendicular to the nuclear symmetry axis,

I is the total angular momentum of the nucleus, a is the decoupling constant, δ is the Kronecker deformation parameter, and K is the projection of I on the axis of symmetry.

The essential features of the extreme shell and collective models are combined in the deformed shell, or Nilsson, model.⁷ Nucleons move in a deformed anisotropic harmonic oscillator potential with cylindrical symmetry; collective excitations are also considered. The energy states are identified⁸ by six asymptotic quantum numbers $\Omega\pi [N, n_z, \Lambda]$, and Σ . Ω is the projection of the total particle angular momentum on the nuclear symmetry axis, π is the parity, N is the total oscillator quantum number, n_z is the number of oscillator quanta along the symmetry axis, Λ is the component of the total orbital angular momentum along the symmetry axis, and Σ is the component of the intrinsic spin s on the symmetry axis. The Nilsson model satisfactorily explains the spectra of low-lying states of most nuclei.⁸

Such a model is, however, not the final answer because it is phenomenological. What is desired is a microscopic theory which explains the observed properties of the unified Nilsson model by the known properties of the nuclear force. No consistently microscopic model yet exists, since phenomenological parameters are still used. Still, much progress has been made in the last decade.⁸

The superfluid model of the nucleus takes into account the residual nucleon-nucleon interactions that are left after the average nuclear potential has been considered. These residual interactions are pair correlations of the superconducting type and multipole-multipole interactions.⁹ The nuclear Hamiltonian is divisible into five parts:¹⁰

$$H = H_{av} + H_{pair} + H_{coll} + H_{rot} + H_c \quad (3)$$

The average field of the nucleus is represented by H_{av} . H_{pair} and H_{coll} are the residual nucleon interactions, where H_{pair} is the interaction leading to pairing correlations and H_{coll} denotes the multipole-multipole interaction responsible for a number of collective nuclear properties. H_{rot} describes the kinetic energy of rotation and H_c , the Coriolis interaction, is defined as

$$H = \frac{c^2}{2I} (\vec{I}\vec{J}) \quad (4)$$

where I is again the moment of inertia, \vec{I} the total angular momentum, and \vec{J} the momentum of internal motion.

A variational solution for the pairing correlation in the nuclear ground state in the case of non-degenerate orbitals can be expressed in the language of second quantization:¹¹

$$\phi_0 = \prod_{\nu} (u_{\nu} + v_{\nu} a_{\nu}^{\dagger} a_{\bar{\nu}}^{\dagger} |0\rangle.$$

ν and $\bar{\nu}$ denote the single particle orbitals (jm) and $(j-m)$.

A single particle level ν is either completely empty, for which the probability is U_ν^2 , or filled with a pair of like nucleons, for which the probability is V_ν^2 . a_ν^+ defines a creation operator operating on the vacuum $|0\rangle$ and creating a particle in the shell model orbit Ψ_ν and

$$a_\nu^+|0\rangle = (-)^{\nu} \Psi_\nu \quad (6)$$

The energy of the pair of particles in the orbital ν is

$$E_\nu = \sqrt{(\varepsilon_\nu - \lambda)^2 + \Delta^2} \quad (7)$$

where ε_ν is the single-particle energy, λ is very nearly equal to the Fermi energy, and Δ gives a measure of the diffuseness of the Fermi surface.

Excited states are discussed in terms of the quasiparticle concept^{1,2}. The ground state is defined as the quasiparticle vacuum $|\bar{0}\rangle$. All excitations are expressed relative to this ground state by quasiparticle operators

$$a_\nu^+ = U_\nu a_\nu^+ - V_\nu a_{\bar{\nu}} \quad (8)$$

$$a_{\bar{\nu}} = U_\nu a_{\bar{\nu}} + V_\nu a_\nu$$

In even-even systems the lowest excited states are two-quasiparticle states. An excited state $a_\nu^+ a_{\bar{\nu}}^+ |\bar{0}\rangle$, necessarily referring to one kind of particle, corresponds to an energy relative to the ground state equal to $E_\nu + E_{\bar{\nu}}$, $\approx 2\Delta$. Thus no intrinsic excitations are to be found below the gap energy 2Δ for the kind of particles considered.

In even-even, deformed nuclei, the H_{coll} term of the nuclear Hamiltonian, which describes the multipole-multipole interaction, becomes significant⁹ for quadrupole excited states with $K^\pi = 0^+, 2^+$ and octupole states with $K^\pi = 0^-, 1^-, 2^-,$ and 3^- . In the superfluid model the wave functions of the collective states are a superposition of different kinds of two-quasiparticle states. On the basis of the superfluid model Soloviev¹³ has predicted the contributions which two-quasiparticle states can be expected to make to the collective excitations in even-even nuclei.

Single-proton transfer reactions can populate only two-proton quasiparticle states and collective states in the residual nucleus. The purpose of this study is to perform the $^{237}\text{Np}(\alpha, t)^{238}\text{Pu}$ single-proton transfer reaction, determine the differential cross sections of the populated states in the ^{238}Pu nucleus, and measure the contributions of two-proton quasiparticle configurations to the $K^\pi = 0^-$ octupole band. Utilizing additional data from the $^{239}\text{Pu}(d, t)^{238}\text{Pu}$ reaction, the contributions of two-neutron quasiparticle configurations to the $K^\pi = 0^-$ octupole band of ^{238}Pu can also be determined. Finally, these measured contributions will be compared with the contributions predicted by Soloviev.

EXPERIMENTAL PROCEDURE

Beams of 27.5- and 28.0-MeV α particles from the Argonne FN tandem Van de Graaff accelerator were used in these experiments. The ^{237}Np targets were prepared with an electromagnetic isotope separator in the Argonne Chemistry Division.¹⁴ The beam from the separator deposited $\sim 400 \mu\text{g}/\text{cm}^2$ of neptunium directly on to a self-supporting carbon backing, which had a thickness of $\sim 40 \mu\text{g}/\text{cm}^2$. The target material was generally confined to a rectangular area $1 \times 3 \text{ mm}$ to reduce the background in the spectra and limit the total amount of radioactivity present on the target. The latter was useful for reasons of safety. The target was placed in a scattering chamber and positioned in the beam with an external micrometer to maximize the amount of beam scattered into a silicon surface-barrier detector mounted at 90° to the beam while minimizing the scattering from the edges of the target frame.

The tritons ($^3\text{H}^+$ ions) produced by the $^{237}\text{Np}(\alpha, t)^{238}\text{Pu}$ reaction were analyzed with an Enge split-pole magnetic spectrograph¹⁵. For the experiments at 27.5 MeV a spectrograph entrance aperture of 3.14 msr (milliradians) and a magnet frequency of 49.092 MHz were used, while for the 28.0-MeV experiment the aperture was 2.0 msr and the magnet frequency was 49.999 MHz. The tritons were detected by nuclear track

plates (Kodak type NTB 50 μm) placed in the focal plane of the spectrograph. Foils of cellulose triacetate were found necessary to eliminate unwanted background tracks in the spectra. A computer code was used to determine the magnet frequency, plate position, and thickness of foil needed to position the spectra at the desired location on the plates for a given incident energy. The overall energy resolution width for the 27.5-MeV reactions was ~ 50 keV, while for the 28.0-MeV reaction the resolution was ~ 30 MeV.

The output of the monitor detector at 90° to the beam was observed with a multichannel analyzer and was also connected to a single-channel analyzer and scaler. The multichannel analyzer was used in adjusting the target position to minimize scattering from the target frame. The window of the single-channel analyzer was set to measure only the elastically scattered α peak from the neptunium target, and the scaler counted these throughout each experiment. The absolute differential cross section was determined from the known solid angles of the monitor (0.512 msr) and spectrograph and the calculated differential cross section for elastic scattering. The spectrograph was used to record a short exposure of the beam elastically scattered from the target. The absolute cross sections for the long reaction exposures (20000 to 400000 μC) could then be calculated from the ratio of the monitor counts during the long and short runs.

The (α, t) exposures were taken at 90° and 110° observation angles. Because of the low cross sections, some of the exposures required 24 h or more. The plates were scanned with a computer-controlled automatic nuclear-emulsion scanner,¹⁶ and the plate from the 28.0-MeV experiment was scanned by hand with a microscope as well, in 0.25- and 0.50-mm channels. A computer program was written to sum the data in every two adjacent channels of the punched-card output from the automatic scanner. The 0.50-mm spectra were stored on disk in the Argonne Chemistry Division Sigma Five computer and viewed on a Tektronix display screen to choose a reference peak. The reference peak shape was used in the input to the automatic spectrum decomposition program AUTOFIT¹⁷, which ran on the Argonne IBM 370/360 computer. The AUTOFIT code uses a sophisticated least-squares fitting routine to find peaks with a 0.6 or greater probability of correlation.

CALCULATION OF DIFFERENTIAL CROSS SECTIONS

The differential cross section for a stripping or pickup process on a nonspherical target nucleus can be expressed in terms of the Nilsson wave functions and intrinsic single-particle transfer cross sections as obtained from a distorted-wave Born-approximation (DWBA) calculation.¹⁸ For the general case including Coriolis mixing between states, the cross section for a stripping reaction to a final state in an even-even residual nucleus can be written¹⁹

$$\frac{d\sigma^{(+)}}{d\omega} = N^{(+)} \sum_{jl} \sigma_l^{(+)}(\theta) \left[\sum_n \langle I_i j K_i \Delta K^{(n)} | I_f K_f^{(n)} \rangle U_n \alpha_n C_{jl}^{(n)} \right]^2 \quad (9)$$

where $d\sigma^{(+)}/d\omega$ is the differential cross section to a member of rotational band l , $N^{(+)}$ is the normalization constant, $\sigma_l^{(+)}(\theta)$ is the DWBA single-particle cross section, I_i and I_f are the target and final-state spins, K_i and $K_f^{(n)}$ are the values of angular momentum projection along the nuclear symmetry axis for the initial and final states, j is the total angular momentum of the transferred proton, the U_n are the pairing emptiness factors for the n wave functions contributing to the given level, α_n are the amplitudes of the individual contributions from other bands, and the $C_{jl}^{(n)}$ are the expansion coefficients of the Nilsson wave functions contributing to the level of the captured proton.

The DWBA single-particle cross sections $\sigma^{(+)}(\theta)$ were calculated with the computer code DWUCK²⁰, using the optical-model parameters given by Wildenthal *et al*²¹ and Lilley

et al²². Differential cross sections from the experimental spectra were computed using the code AUTO PLOT. Theoretical differential cross sections, including the effects of Coriolis band mixing, were computed with the program BANDMIX.²³

EXPERIMENTAL RESULTS

Spectra from $^{239}\text{Pu}(d,t)^{238}\text{Pu}$ reactions at 12.0 MeV performed by Arnold Friedman and Kenji Katori²⁴ were made available for comparison with the (α,t) spectra. Typical spectra from the (d,t) and (α,t) reactions are shown on the same excitation energy scale in Fig. 1. The spectrum from the (α,t) reaction at 27.5 MeV and an observation angle of 90° is shown in Fig. 2, while Fig. 3 shows the spectrum from the 27.5-MeV (α,t) reaction at a 110° observation angle. Table I lists the excitation energies, measured absolute differential cross sections, and assignments made to the levels of ^{238}Pu . An energy level diagram of ^{238}Pu which includes all assignments made from the present study is presented in Fig. 4.

DISCUSSION

Energy levels in ^{238}Pu were identified using theoretical differential cross sections and rotational spacings calculated for intrinsic two-quasiparticle excitations using the computer code BANDMIX^{2,3}. Coriolis mixing of bands was taken into account in these calculations. Calculated contributions of two-quasiparticle excitations to collective bands in ^{238}Pu are presented in TABLE II. In most cases only the even or the odd spin members of the rotational bands are seen in the spectra. Thus it is assumed that the total differential cross section seen in one of these intrinsic excitation rotational bands is half of the total differential cross section of the intrinsic excitation.

The calculated contribution of the $K^\pi = 5^-$ two-quasiparticle band in the (α, t) reaction to the $K^\pi = 0^-$ octupole band in ^{238}Pu is $12\% \pm 2\%$. The contribution of this configuration predicted by Soloviev is 18 %. Thus the superfluid model calculation by Soloviev^{1,3} yields a relatively accurate value for the contribution of the $\frac{5}{2} + [642]\pi, \frac{5}{2} \pm [523]\pi$ two-quasiparticle configuration to the $K^\pi = 0^-$ octupole band of ^{238}Pu .

REFERENCES AND FOOTNOTES

¹M. G. Mayer, Phys. Rev. 74, 235 (1948); 75, 1969 (1949); 78, 16 (1950).

²O. Haxel, J. H. D. Jensen, and H. Suess, Phys. Rev. 75, 1766 (1949); Z. Physik 128, 295 (1950).

³J. H. Bartlett, Phys. Rev. 41, 370 (1932); W. M. Elsasser, J. Phys. Radium 4, 549 (1933); 5, 625 (1934).

⁴A. Bohr, Phys. Rev. 81, 134 (1951); A. Bohr and B. R. Mottelson, Kgl. Danske Videnskab. Selskab. Mat.-fys. Medd. 27, No. 16 (1953).

⁵A. Bohr, Dan. Mat.-fys. Medd. 26, No. 14 (1952).

⁶E. K. Hyde, I. Perlman, and G. T. Seaborg, The Nuclear Properties of the Heavy Elements, Vol. 1, Prentice-Hall, Inc., Englewood Cliffs, New Jersey, 1964, p. 92.

⁷S. G. Nilsson, Dan. Mat.-fys. Medd. 29, No. 16 (1955).

⁸H. Frauenfelder and E. M. Henley, Subatomic Physics, Prentice-Hall, Inc., Englewood Cliffs, New Jersey, 1974, p. 433.

⁹V. G. Soloviev, in Structure of Complex Nuclei, N. N. Bogolyubov, ed., Plenum Publishing Corporation, New York, 1969, p. 23.

¹⁰V. G. Soloviev, At. Energy Rev. 3, 117 (1965).

¹¹Bohr, Mottelson, and Pines, Phys. Rev. 110, 936 (1958).

¹²N. N. Bogoliubov, JETP 7, 41 (1958); Nuovo Cimento 7, 794 (1958); J. G. Valatin, Nuovo Cimento 7, 843 (1958).

¹³V. G. Soloviev and T. Siklos, Nucl. Phys. 59, 145 (1964).

¹⁴We are indebted to J. Lerner for the preparation of these targets.

¹⁵J. E. Spencer and H. A. Enge, Nucl. Instrum. Methods 49, 181 (1967).

¹⁶J. R. Erskine and R. H. Vonderohe, Nucl. Instrum. Methods 81, 221 (1970).

¹⁷P. Spink and J. R. Erskine, Argonne National Laboratory Physics Division Informal Report No. PHY-1965B (unpublished); J. R. Comfort, Argonne National Laboratory Physics Division Informal Report No. PHY-1970B (unpublished).

¹⁸G. R. Stachler, Ann. Phys. (N. Y.) 3, 275 (1958); S. S.

¹⁹B. Elbek and P. O. Tjøm, in Advances in Nuclear Physics, Vol. 3, M. Baranger and E. Vogt, ed., Plenum Publishing Corporation, New York, 1969, p. 259.

²⁰We are grateful to Dr. P. D. Kunz for making this code available to us.

²¹B. H. Wildenthal, B. M. Freedom, E. Newman, and M. R. Cates, Phys. Rev. Letters 19, 960 (1967).

²²J. S. Lilley and N. Stein, Phys. Rev. Letters 19, 709 (1967).

²³J. R. Erskine and W. W. Buechner, Phys. Rev. 133, B370 (1964).

²⁴Unpublished.

²⁵Y. A. Ellis, Nucl. Data Sheets 4, 637 (1970).

TABLE I. Energy levels in ^{238}Pu , their orbital assignments, their excitation energies, and their differential cross sections observed with the (α, t) and (d, t) reactions.

Assignment of level		Excitation energy	$d\sigma(d, t)/d\omega$	$d\sigma(\alpha, t)/d\omega$	($\mu\text{b}/\text{sr}$)		
Configuration ^a	K^π	I^π	energy (keV)	$E_I = 12.0$ MeV	$E_I = 28.0$ MeV	$E_I = 27.5$ MeV	
			($\mu\text{b}/\text{sr}$)	90°	90°	110°	
	0^+	0^+	0.0^d	38.9 ± 2.3	0.2 ± 0.1	0.1 ± 0.1	0.3 ± 0.1
	2^+	2^+	44.1 ± 0.1^d	102.3 ± 7.2	0.9 ± 0.1	1.0 ± 0.1	0.7 ± 0.1
	4^+	4^+	146.0 ± 0.2^d	38.9 ± 2.6	2.6 ± 0.1	2.7 ± 0.1	1.7 ± 0.1
	6^+	6^+	303.6 ± 0.5^d	1.7 ± 0.4	5.6 ± 0.1	5.4 ± 0.2	3.6 ± 0.1
	8^+	8^+	$514. \pm 2. ^d$		1.0 ± 0.1	1.0 ± 0.1	1.9 ± 0.1
oct-vib	0^-	1^-	604.9 ± 0.1^d	7.6 ± 0.8	0.8 ± 0.1	0.4 ± 0.1	0.3 ± 0.1
	3^-	3^-	661.3 ± 0.1^d	5.2 ± 0.9	1.8 ± 0.1	1.6 ± 0.1	1.3 ± 0.1
	5^-	5^-	769.4 ± 2.5	2.7 ± 0.5	0.9 ± 0.1	0.9 ± 0.1	0.7 ± 0.1
b			834.8 ± 0.7	2.2 ± 0.2			
β -vib	0^+	0^+	942.8 ± 1.8	2.2 ± 0.5			
	2^+	2^+	984.7 ± 1.0	6.5 ± 0.6			
c			961.3 ± 2.5	1.8 ± 0.5	0.8 ± 0.2	0.6 ± 0.1	0.6 ± 0.1

TABLE I. (Continued)

γ -vib	2^+	2^+	1028.3 ± 0.5^d	13.1 ± 1.2	2.0 ± 0.3	1.6 ± 0.2	1.0 ± 0.2
	3^+	3^+	1069.7 ± 0.5^d	24.4 ± 2.0	1.3 ± 0.2	0.9 ± 0.2	0.9 ± 0.1
	4^+	4^+	1130.1 ± 3.2	6.0 ± 0.8			
	5^+	5^+	1195.8 ± 0.6	11.8 ± 0.9			
$\frac{1}{2} + [631] \nu$	2^+	2^+	1143.2 ± 2.0	8.9 ± 0.9			
$\frac{5}{2} + [633] \nu$	3^+	3^+	1177.9 ± 0.4	15.5 ± 1.1			
	4^+	4^+	1239.1 ± 3.8	1.2 ± 0.8			
	5^+	5^+	1289.7 ± 0.5	14.0 ± 1.2			
			1160.4 ± 13.8			0.2 ± 0.1	0.2 ± 0.1
			1236.8 ± 6.9		1.2 ± 0.2	1.0 ± 0.1	0.9 ± 0.1
			1251.5 ± 3.6	4.7 ± 1.0			
			1264.5 ± 2.5	2.8 ± 0.8			
$\frac{5}{2} + [642] \pi$	5^+	5^+	1295.0 ± 1.2		3.7 ± 0.3	3.2 ± 0.2	2.9 ± 0.2
$\frac{5}{2} - [523] \pi$	6^+	6^+	1367.6 ± 6.8		4.8 ± 0.3	3.8 ± 0.2	3.3 ± 0.2
	7^+	7^+	1452.9 ± 3.0		4.2 ± 0.3	4.6 ± 0.2	4.2 ± 0.2
			1344.0 ± 0.8	4.8 ± 0.7			
			1361.6 ± 1.6	3.1 ± 0.6			

TABLE I. (Continued)

$\frac{1}{2} + [631] \nu$	2^+	2^+	1408.9 ± 0.4	3.1 ± 0.2	
$\frac{3}{2} + [631] \nu$	c	3^+	1450.0 ± 0.5	21.0 ± 2.0	
		4^+	1506.0 ± 3.9	4.3 ± 1.0	
		5^+	1580.0 ± 5.0	1.1 ± 0.8	
			1498.8 ± 3.2		1.3 ± 0.2
			1529.8 ± 4.0	4.0 ± 1.0	
			1545.6 ± 1.3	5.2 ± 1.1	
			1562.9 ± 6.8		0.7 ± 0.1
			1602.3 ± 9.0		1.1 ± 0.2
			1608.2 ± 2.8	3.7 ± 1.0	
c			1623.9 ± 1.1	9.0 ± 1.3	
			1626.0 ± 4.5		1.0 ± 0.1
			1639.1 ± 6.5		0.8 ± 0.2
			1645.3 ± 1.0	9.4 ± 1.3	
			1676.6 ± 1.0	12.8 ± 1.4	
			1695.6 ± 0.3	40.6 ± 2.3	

TABLE I. (Continued)

$\frac{1}{2} + [631] \nu, e 0^- 1^-$	1728.2 ± 0.3	66.6 ± 2.9	
$\frac{1}{2} - [501] \nu$	3^- 1781.3 ± 0.6	13.5 ± 1.0	0.2 ± 0.1
	1731.0 ± 14.1		0.1 ± 0.1
	1742.2 ± 0.9	15.4 ± 1.7	
$\frac{1}{2} + [631] \nu, e 1^- 1^-$	1834.0 ± 0.5	48.9 ± 3.4	
$\frac{1}{2} - [501] \nu$	2^- 1846.2 ± 0.4	48.7 ± 3.4	
	3^- 1897.6 ± 0.7	18.7 ± 2.1	
$\frac{1}{2} + [631] \nu, 0^- 0^-$	1884.5 ± 0.3	38.8 ± 2.7	
$\frac{1}{2} - [501] \nu$	2^- 1920.3 ± 0.4	20.9 ± 2.0	6.5 ± 0.2
	1894.2 ± 19.5		0.9 ± 0.1
	1960.3 ± 0.5	12.4 ± 1.1	
	1974.2 ± 1.2	5.6 ± 0.9	
	1996.8 ± 1.2	4.1 ± 0.8	
	2032.6 ± 0.9	7.5 ± 1.5	
	2067.1 ± 0.4	16.6 ± 1.6	
	2096.1 ± 2.5		2.4 ± 0.4

TABLE I. (Continued)

2099.3 ± 1.0	4.6 ± 1.3	
2133.0 ± 3.0	5.1 ± 1.1	
2150.2 ± 5.2		1.7 ± 0.4
2194.8 ± 7.4		1.0 ± 0.3

^aAll members of the same rotational band are grouped together. The $\frac{1}{2} + [631] \nu, \frac{3}{2} + [631] \nu$ assignment is tentative.

^bThis peak, not present in (α, t) spectra recorded at other angles, is probably caused by a contaminant in the plutonium target used for the reaction.

^cPart or all of the cross sections of these peaks is due to radioactive decays.

^dLiterature values are presented for these well-established energy levels.^{2,5}

TABLE II. Cross sections of collective bands in ^{238}Pu .

Collective Band	Total $d\sigma/d\omega$ in Collective Band ($\mu\text{b}/\text{sr}$)	Total $d\sigma/d\omega$ in Two-Quasiparticle Band ($\mu\text{b}/\text{sr}$)	Total Two-Quasi-particle $d\sigma/d\omega$ in Collective Band ($\mu\text{b}/\text{sr}$)	% of Two-Quasi-particle $d\sigma/d\omega$ in Collective Band
oct-vib $K^\pi = 0^-$		$\frac{5}{2} + [642]_{\pi, \frac{5}{2}} - [523]_{\pi}$ $K^\pi = 5^-$		
(α, t)	3.5 ± 0.3	25.4 ± 1.8	28.9 ± 2.1	12 ± 2
$K^\pi = 0^-$		$\frac{1}{2} + [631]_{\nu, \frac{1}{2}} - [501]_{\nu}$		
(d, t)	15.5 ± 2.2	139.8 ± 8.6	155.3 ± 10.8	(10 ± 13)
β -vib $K^\pi = 0^+$				
(d, t)	8.7 ± 1.1			
γ - vib $K^\pi = 2^+$				
(α, t)	3.3 ± 0.5			
$K^\pi = 2^+$		$\frac{1}{2} + [631]_{\nu, \frac{5}{2}} + [633]_{\nu}$		
(d, t)	55.3 ± 4.9	79.2 ± 8.0	134.5 ± 12.9	41 ± 18

FIGURE CAPTIONS

Fig. 1. Comparison of spectra observed in (a) the reaction $^{239}\text{Pu}(d,t)$ and (b) the reaction $^{237}\text{Np}(\alpha,t)$ to final states in ^{238}Pu . The (d,t) data are from A. M. Friedman and K. Katori²⁴.

Fig. 2. Spectrum observed in the $^{237}\text{Np}(\alpha,t)^{238}\text{Pu}$ reaction at 27.5 MeV and an observation angle of 90° .

Fig. 3. Spectrum observed in the $^{237}\text{Np}(\alpha,t)^{238}\text{Pu}$ reaction at an incident α energy of 27.5 MeV and an observation angle of 90° .

Fig. 4. Energy level diagram of ^{238}Pu . Wherever possible the levels have been assigned to rotational bands whose asymptotic quantum numbers or collective designation are given below each band. The assigned spins for each rotational level are given. The assignment of the $\frac{1}{2} + [631] \nu$, $\frac{3}{2} + [631] \nu$ band is tentative.

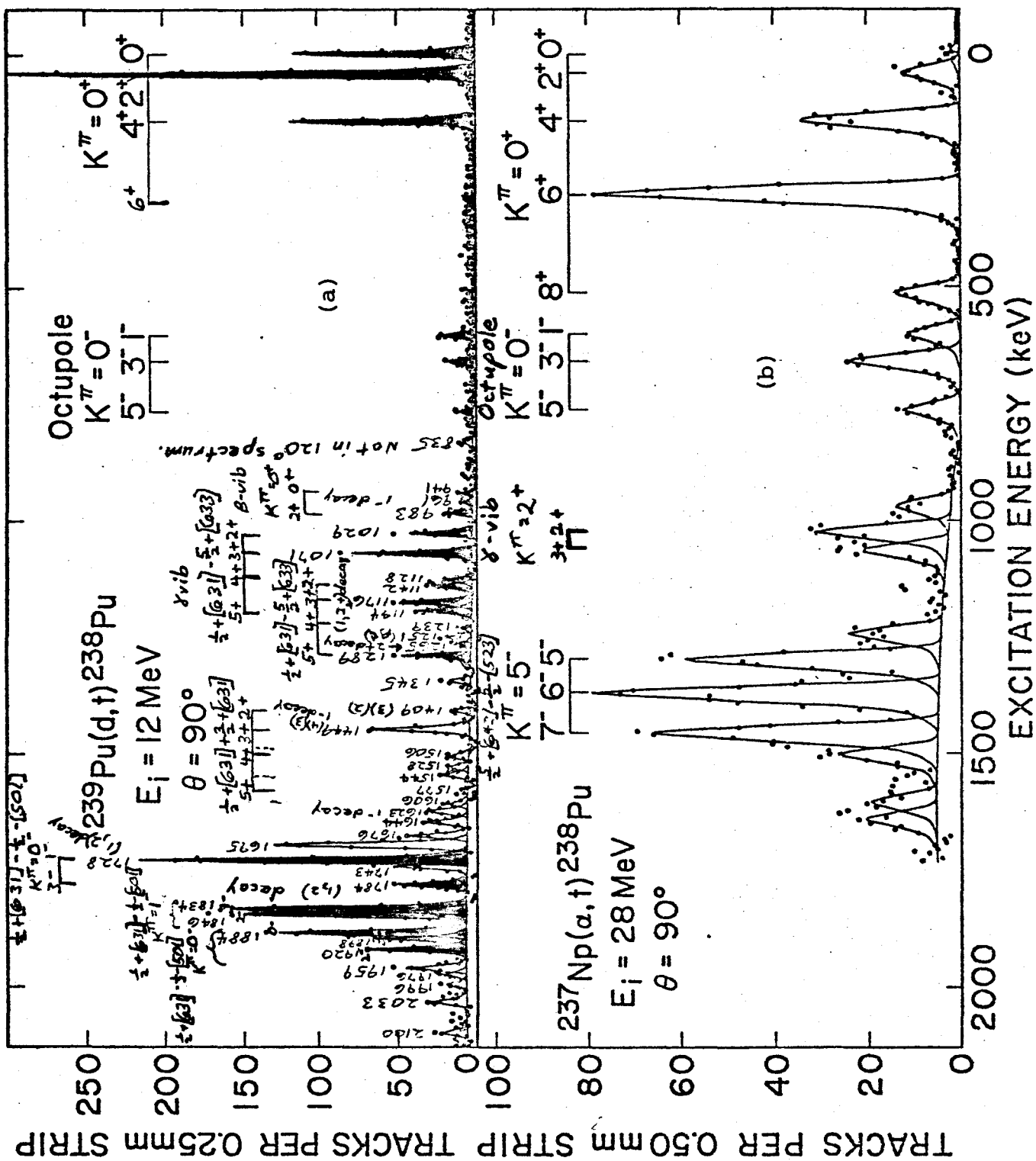


Figure 1.

127-50154

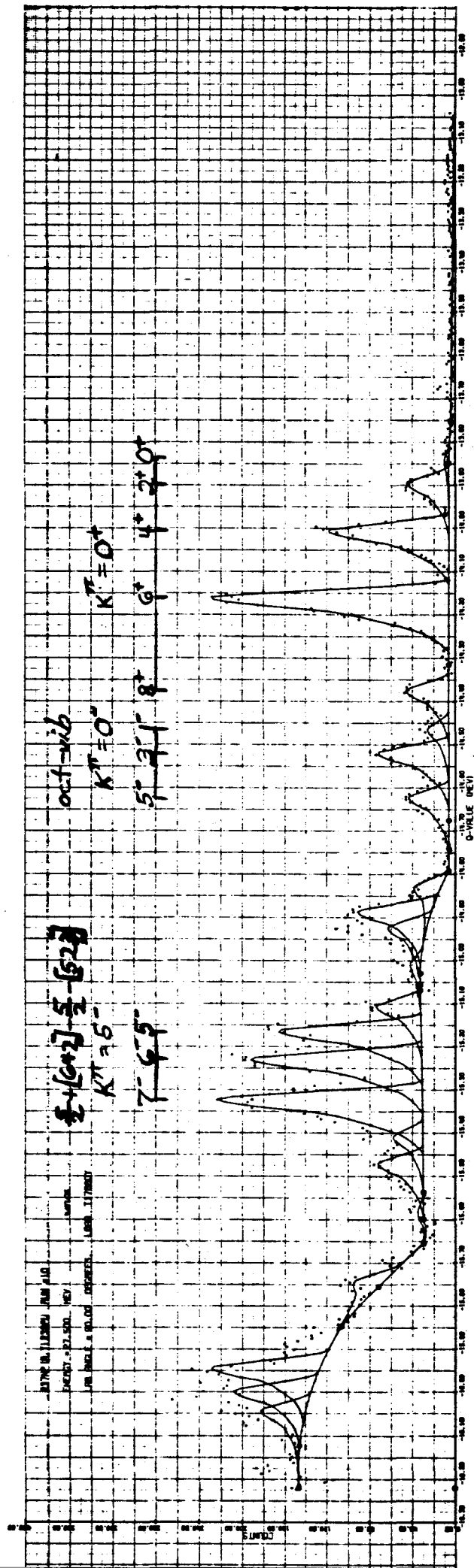


Figure 2.

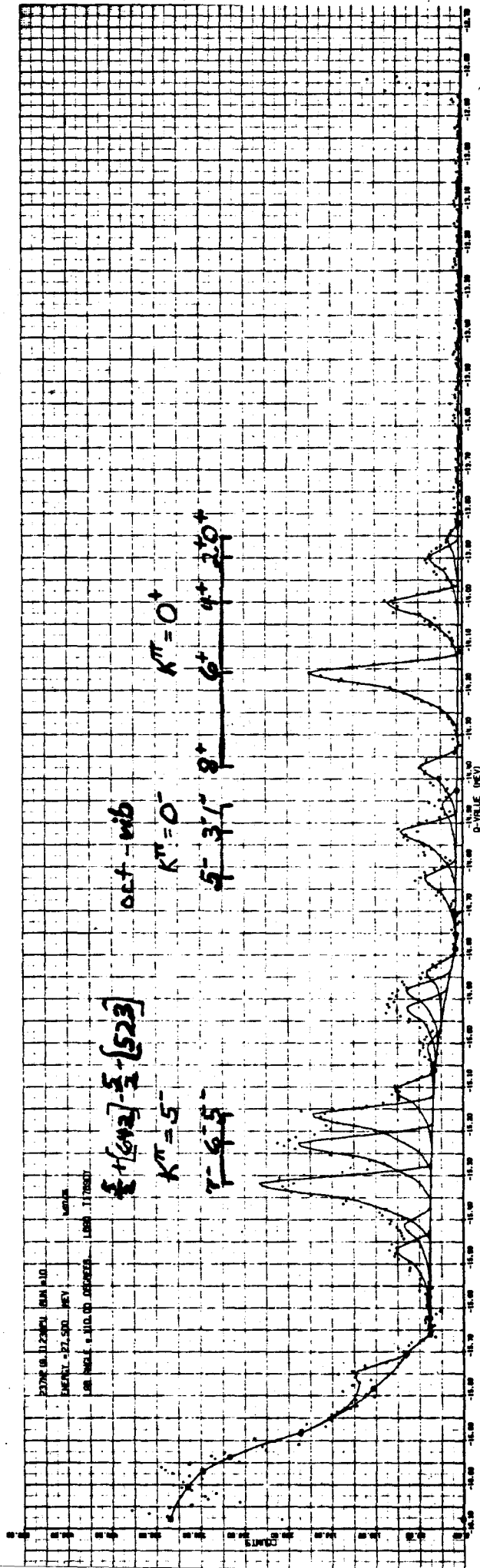


Figure 3.

